International Journal of
Science and Engineering Investigations vol. 9, issue 107, December 2020
Received on December 21, 2020 ISSN: 2251-8843

Thermal Image Analysis of a Cement Kiln Dust Treated Slope

Hamid Ranjkesh Adarmanabadi[1], Arezou Rasti[2], Mehrdad Razavi[3]
[1,2,3]Department of Mineral Engineering, New Mexico Institute of Mining and Technology, Socorro, NM, USA
([1]hamid.ranjkesh@student.nmt.edu, [2]arezou.rasti@student.nmt.edu, [3]mehrdad.razavi@nmt.edu)

Abstract- This study presents the effects of additives such as cement kiln dust (CKD) to stabilize the soil on soil thermal images due to the changes in the treated soil's thermal properties. In Socorro, NM, a natural soil slope treated with different amounts of CKD to reduce erosion in 2008 was selected for this research. The slope was divided into four sections; the 30 cm of the slope surface in these sections was treated with 0%, 5%, 10%, and 15% of CKD (by soil's dry weight). In 2019, a soil pH distribution map of the slope showed traces of CKD concentration in each section and proportional to the CKD concentration in 2008. The slope's thermal images were captured for twelve hours, starting at 6:30 am on an hourly basis. A small-scale test model of the slope was also built in the lab using the untreated native slope soil to increase thermal images' resolution. The test-model was exposed to the outside environment, and the thermal images were captured using the same time capture-schedule of the field slope. The thermal image analysis results of both the field test and the small-scale test revealed the visible changes in the thermal images of different sections treated with different amounts of CKD due to the reduction of thermal diffusivity and improved treated soil's thermal conductivity. This study shows that thermal image analysis is an effective method to detect the treated soils with additives affecting soil thermal properties, such as CKD and the additive concentration in soil, in conjunction with traditional techniques.

Keywords- *Thermal Behavior, Cement Kiln Dust (CKD), Thermal Conductivity, Thermal Imaging Analysis*

I. INTRODUCTION

Soil temperature is an influential parameter affecting plant processes and soil microbial diversity (Sabri et al., 2018). The study of soil thermal behavior is essential since soil thermal properties significantly affect engineering applications (Kang et al., 2015). Several investigations are surveying heat-related problems in geotechnical engineering. It is a significant concern that should be taken into account; for example, it is crucial to know the heat capacity and thermal conductivity of soil to estimate heat transfer in soil. The thermal behavior of soil close to the surface is a fundamental parameter to examine the air-soil interface's energy balance at the ground's surface (Hopmans & Dane, 1986; Kodikara et al., 2011).

The heat flow at any depth in the soil is proportional to the temperature gradient at that point, and the proportionality coefficient is the thermal conductivity. Thermal diffusivity is the ratio of thermal conductivity to volumetric heat capacity (Shiozawa & Campbell, 1990). There are different techniques in order to survey the thermal conductivity of the soil. The single probe method can be used to estimate the thermal conductivity of the soil. Abu-Hamdeh and Reeder (2000) followed a laboratory experiment to survey the thermal conductivity of sand, sandy loam, loam, and clay loam using the single probe method. Ochsner et al. (2001) investigated the soil thermal properties by using the heat-pulse method. Heat capacity, thermal diffusivity, and thermal conductivity are parameters that were surveyed in their study. They concluded that the volume fraction of water, volume fracture of solids, and volume fraction of air in the soil are crucial parameters affecting the soil thermal properties.

The Decagon Devices KD2 Pro Thermal Properties Analyzer is another method employed by Kang et al. (2015) to record all the soil's thermal conductivities. Kodikara et al. (2011) highlighted the application of thermal imaging for geotechnical engineering investigations. Additionally, they suggested that thermal imaging can be effectively used to estimate the soil's thermal diffusivity in the laboratory.

Thermal diffusivity of soil can be measured directly and indirectly by using several different techniques. Besides, various methods were suggested to estimate soil's thermal properties by recording the field's temperature. Thermal imaging is a method of converting an object's visible radiation pattern (e.g., soil) into visible images. Thermal imaging is a non-contact and non-destructive technique that has many applications due to its ease of use. It can produce an overall picture of the temperature distribution on the subjects and provide an accurate temperature of the surface viewed (Kodikara et al., 2011). The thermal camera converts the invisible infrared radiation released by subjects into temperature and displays as thermal images (Rao, 2008).

Chemical additives such as cement, cement kiln dust (CKD), and lime can improve soil formations' engineering properties (Faramarzi et al., 2016). Various investigators have reported the effect of additives material on soil's thermal behavior; for example, Folaranmi (2009) determined the effect of different amounts of fly ash and sawdust on clay's thermal conductivity. The study results showed that additive material such as ashes, sawdust, animal dung, and bentonite improve clay's thermal conductivity. Edet et al. (2017) investigated the effect of additives on Loamy soil's thermal conductivity in Calabar, Nigeria. The result of their study reveals that the thermal conductivity of Loamy soil increases with additives.

The effect of cement content on the thermal conductivity of cement stabilized earth blocks was investigated by Zhang et al. (2017). Quartz, calcite, anorthite, and albite stabilized with Portland cement, and the thermal conductivity of prepared specimens was measured by the hot disk apparatus method. The results demonstrated an increase in the thermal conductivity of the stabilized soil. Besides, adding cement causes a decrease in soil porosity, explaining the increase in stabilized soil's thermal conductivity (Zhang et al., 2017).

An experimental study surveyed the effect of salt concentration on the thermal conductivity of different soils. For this purpose, different amounts of NaCl and $CaCl_2$ were added to sand, sandy loam, loam, and clay loam soils. The single probe methodology was used to measure treated specimens' thermal conductivity in different moisture content and bulk density. All specimens were air-dried and sieved through a 0.2 cm sieve. The results indicated that thermal conductivity increased by increasing the bulk density and moisture content and decreased by increasing the salt concentration (Abu-hamdeh & Reeder, 2000).

To the best of the authors' knowledge, no studies have been done on the treated soil's thermal behavior using the thermal imaging method yet. In this study, the thermal imaging method is used to survey the effect of additives on stabilized soil's thermal behavior. For this reason, the natural slope stabilized by CKD was selected. The thermal behavior of the slope was monitored by using a thermal camera. Besides, similar tests were conducted on a small-scale slope built in the lab exposed to the outside temperature. The thermal behavior of treated soil with different amounts of CKD was examined using the thermal imaging camera to compare the field and laboratory results.

II. Methodology

A natural slope stabilized with CKD in 2008 located in Socorro, NM, was selected for this study. The slope was divided into four sections, and 30 cm of the slope surface was stabilized with 0%, 5%, 10%, and 15% of CKD to determine the effect of CKD to reduce the soil erosion. Figure 1 shows a schematic isometric view of the slope and sections stabilized with different amount of CKD. Figure 2 presents the effect of different CKD contents on soil's pH. In 2019, a soil pH distribution map of the slope showed traces of CKD concentration in each section and proportional to the CKD concentration in 2008 (Figure 3). It was indicated that section 4 was stabilized with 15% of CKD recorded the highest pH and CKD concentration. A commercial thermal camera (Fluke Ti450 Pro) was used to take the slope's thermal images at different times (Figure 4). The sensitivity of the thermal camera is less than 0.025 at 30 centigrade target temperature. The camera creates a 640×480 image. Thermal images of the slope surface were recorded hourly. The duration of this survey was from 6:30 am to 8:30 pm. Besides, each sections' surface temperature was recorded at different points for each section, and a mean value was assigned for the surface temperature of each section at different times.

A small-scale slope was made to evaluate CKD's effect on soil's thermal conductivity in the lab to compare the field and lab results. The soil used to make a slope in the lab was taken from the untreated part of the natural slope. For this purpose, different CKD amounts were added to soil to model the natural slope in the lab. The first section from the left is untreated native soil. Sections two through four were stabilized with 5%, 10%, and 15% CKD (by the soil's dry weight), respectively. Figure 5 shows a schematic isometric view of the slope built in the lab and treated with different CKD amount. The thermal behavior of the prepared slope in the lab was studied from 6:30 am to 8:30 pm hourly, and the surface temperature of the slope's section was recorded.

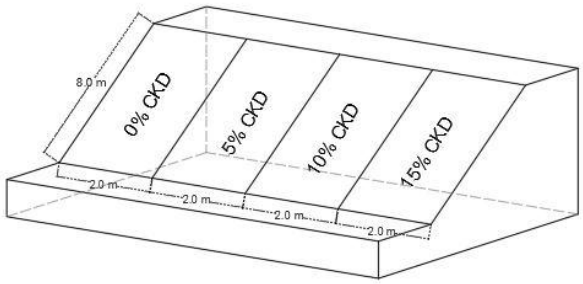

Figure 1. A schematic isometric view of the slope in the field and CKD content of each section at the treatment time in 2008

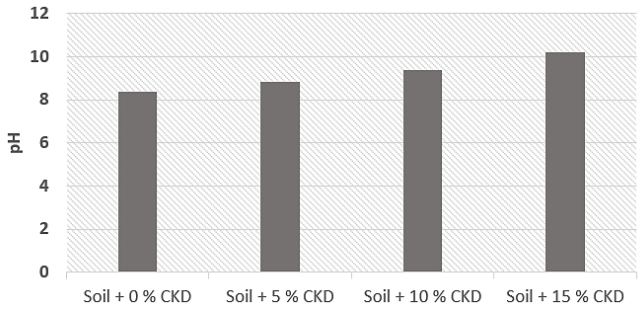

Figure 2. Soil pH at different CKD content

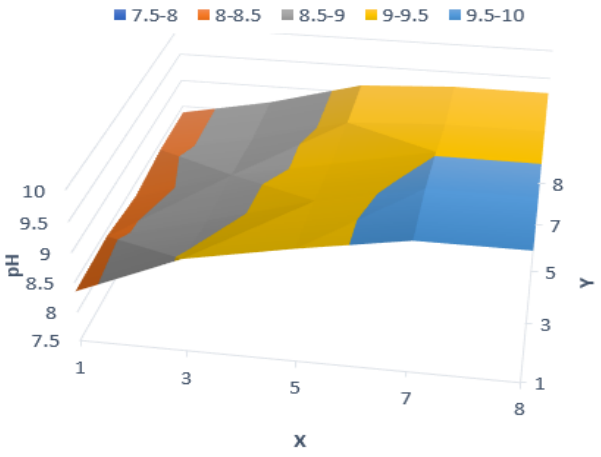

Figure 3. CKD distribution on the slope in 2019

Figure 4. Thermal camera (Fluke Ti450 Pro; www.fluke.com)

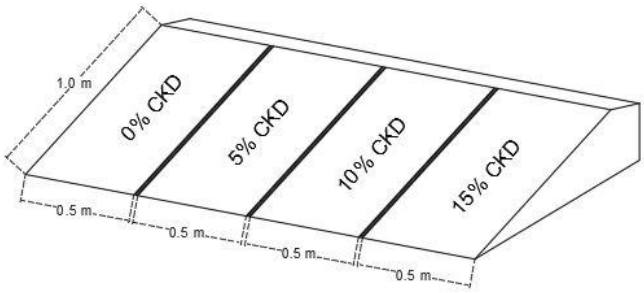

Figure 5. An isometric view of the small-scale model of the slope profile in laboratory

III. RESULT AND DISCUSSION

This investigation aims to survey the thermal behavior of stabilized soil with CKD and the additive footprints on the thermal images. The slope was divided into four sections, and it was stabilized with 0, 5%, 10%, and 15% CKD (from left to right), respectively, in 2008. Figure 6 to figure 20 show the slope's thermal images taken with the thermal camera from 6:30 am to 8:30 pm.

In figure 6 through figure 20, the areas with a higher amount of CKD show a lower temperature. This trend is observed in all thermal images of the slope at different times. The temperature distribution pattern follows the distribution of CKD in different sections. It is important to note that the irregularity in temperature in the treated sections is due to particles' migration by wind, rain, and surface runoff. Similar results were obtained for the small-scale test model (Figure 21 through figure 35). However, the scatter or irregularities in temperature distribution is less as the CKD distribution in each section is uniform. The results of the small-scale slope verify the results of the field slope as well.

The different surface temperatures that change with the CKD concentration show that CKD affects soil's thermal behavior. It means that CKD increases the conductivity of the soil. It can be concluded that CKD reduced the thermal diffusivity of soils. The same behavior is anticipated for similar additives such as cement.

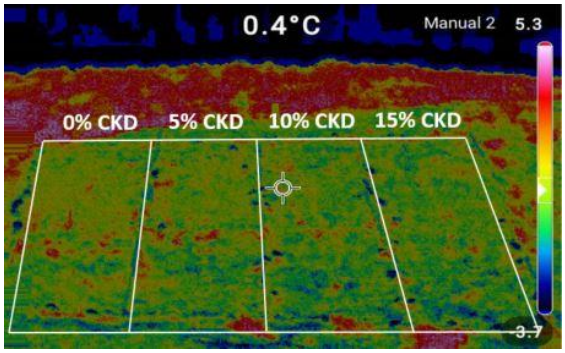

Figure 6. A thermal image of the slope showing the temperature on the slope surface at 6:30 am

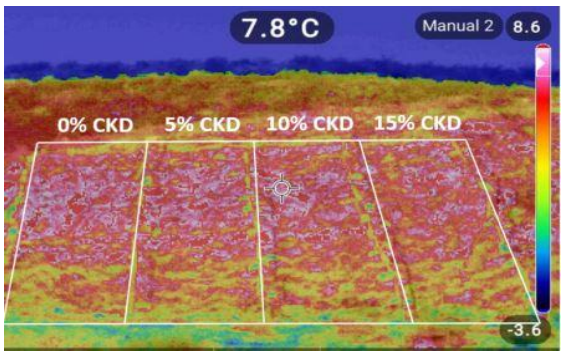

Figure 7. A thermal image of the slope showing the temperature on the slope surface at 7:30 am

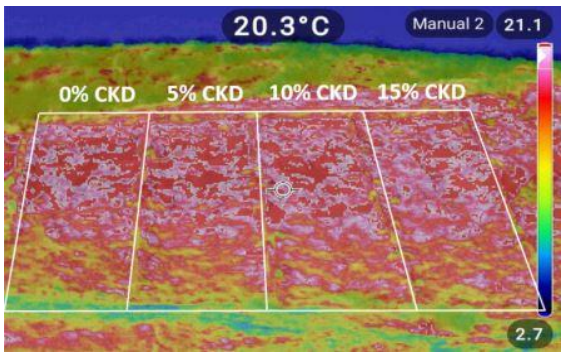

Figure 8. A thermal image of the slope showing the temperature on the slope surface at 8:30 am

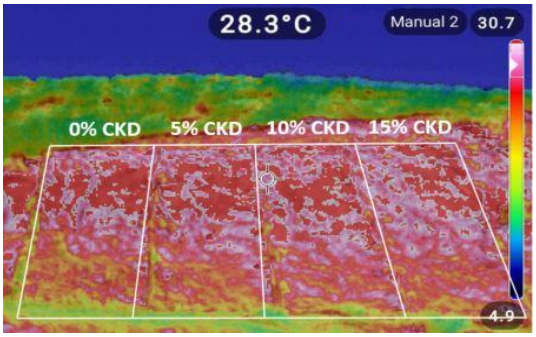

Figure 9. A thermal image of the slope showing the temperature on the slope surface at 9:30 am

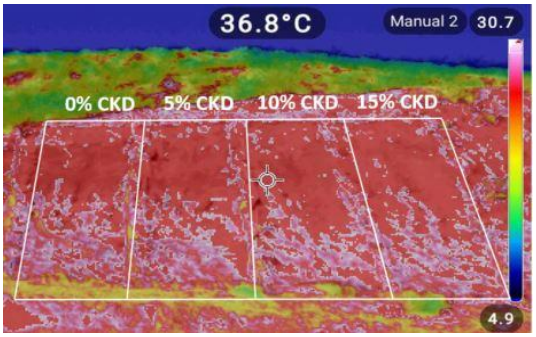

Figure 10. A thermal image of the slope showing the temperature on the slope surface at 10:30 am

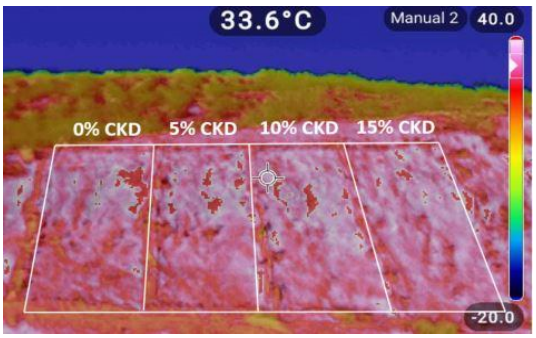

Figure 11. A thermal image of the slope showing the temperature on the slope surface at 11:30 am

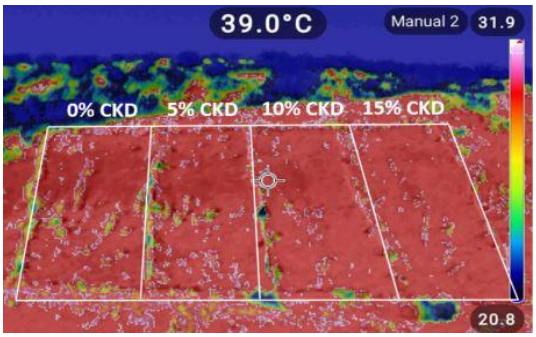

Figure 12. A thermal image of the slope showing the temperature on the slope surface at 12:30 pm

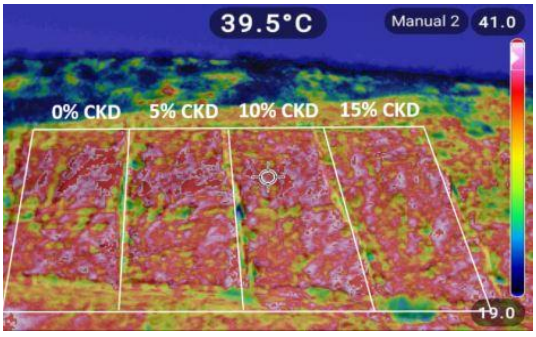

Figure 13. A thermal image of the slope showing the temperature on the slope surface at 1:30 pm

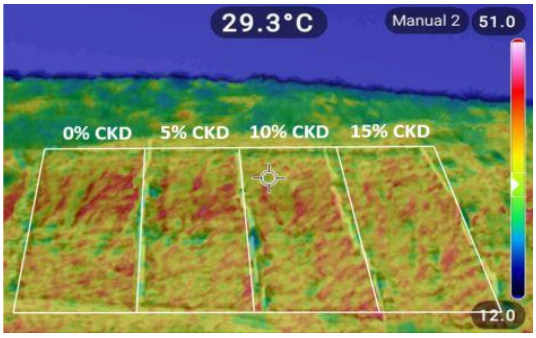

Figure 14. A thermal image of the slope showing the temperature on the slope surface at 2:30 pm

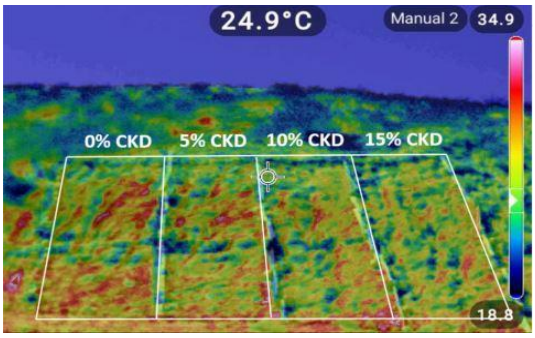

Figure 15. A thermal image of the slope showing the temperature on the slope surface at 3:30 pm

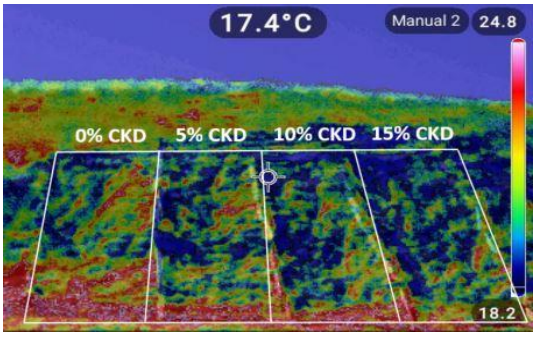

Figure 16. A thermal image of the slope showing the temperature on the slope surface at 4:30 pm

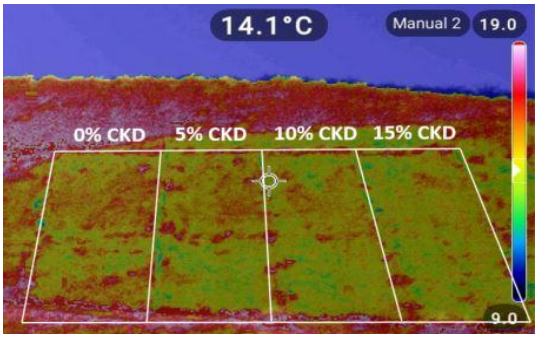

Figure 17. A thermal image of the slope showing the temperature on the slope surface at 5:30 pm

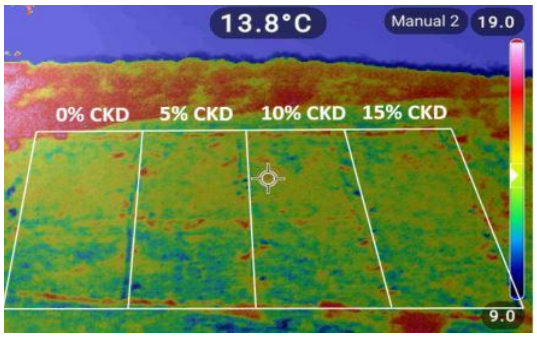

Figure 18. A thermal image of the slope showing the temperature on the slope surface at 6:30 pm

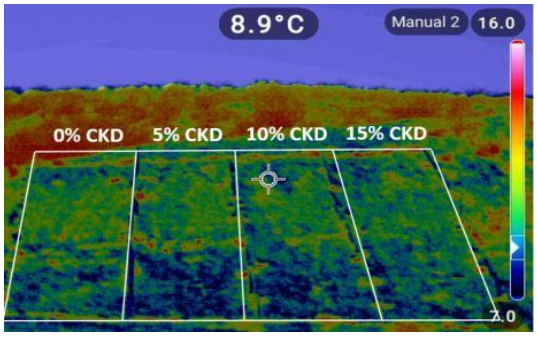

Figure 19. A thermal image of the slope showing the temperature on the slope surface at 7:30 pm

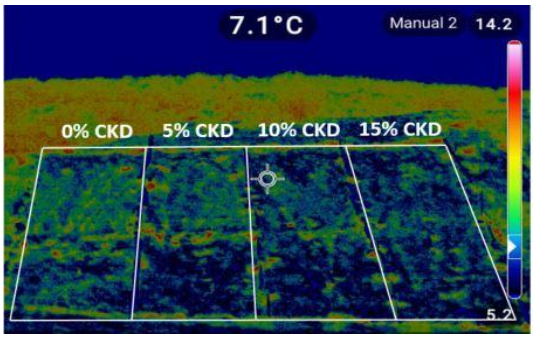

Figure 20. A thermal image of the slope showing the temperature on the slope surface at 8:30 pm

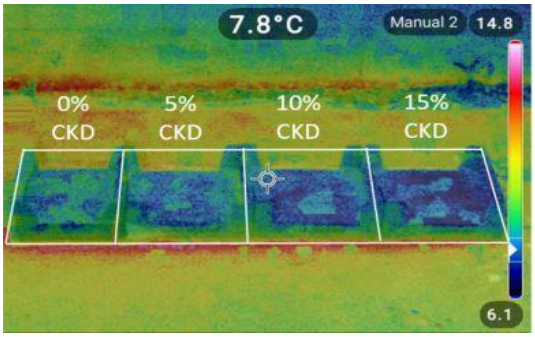

Figure 21. A thermal image of the small-scale model of the slope showing the temperature on the surface at 6:30 am

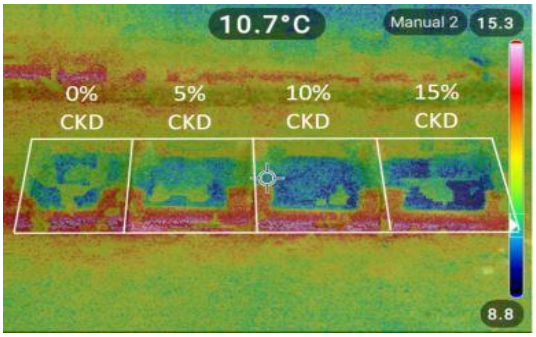

Figure 22. A thermal image of the small-scale model of the slope showing the temperature on the surface at 7:30 am

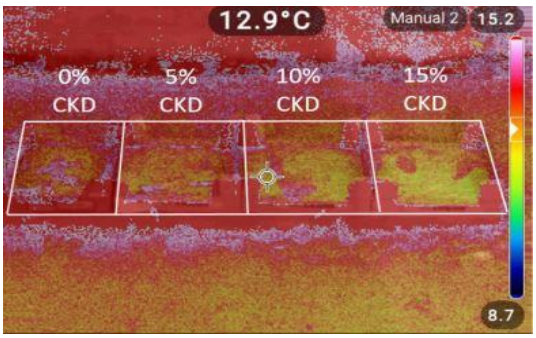

Figure 23. A thermal image of the small-scale model of the slope showing the temperature on the surface at 8:30 am

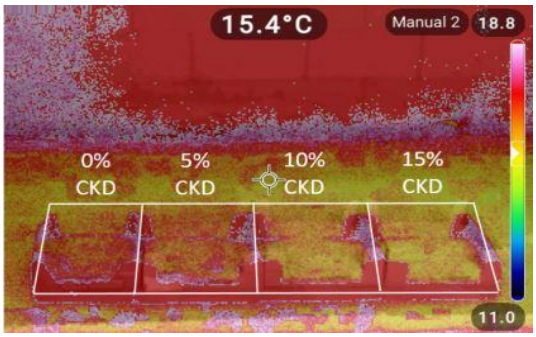

Figure 24. A thermal image of the small-scale model of the slope showing the temperature on the surface at 9:30 am

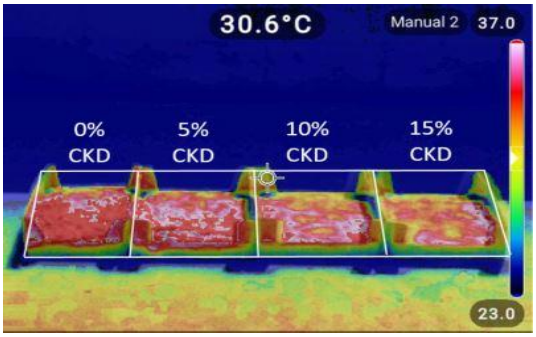

Figure 25. A thermal image of the small-scale model of the slope showing the temperature on the surface at 10:30 am

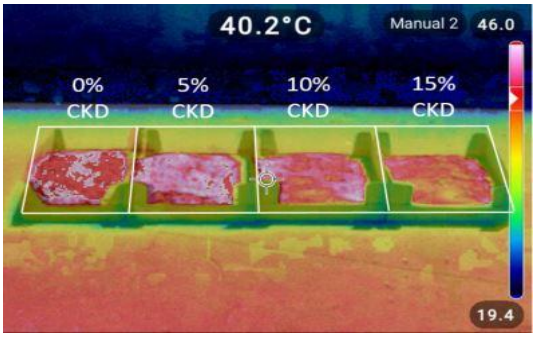

Figure 26. A thermal image of the small-scale model of the slope showing the temperature on the surface at 11:30 am

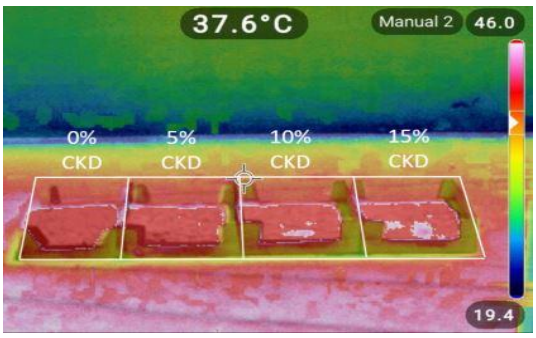

Figure 27. A thermal image of the small-scale model of the slope showing the temperature on the surface at 12:30 pm

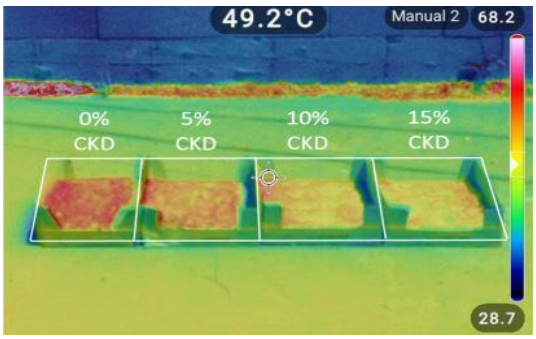

Figure 28. A thermal image of the small-scale model of the slope showing the temperature on the surface at 1:30 pm

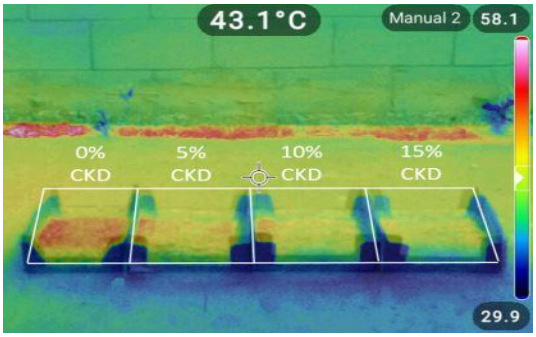

Figure 29. A thermal image of the small-scale model of the slope showing the temperature on the surface at 2:30 pm

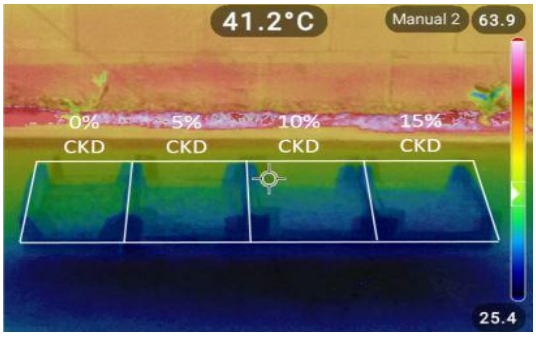

Figure 30. A thermal image of the small-scale model of the slope showing the temperature on the surface at 3:30 pm

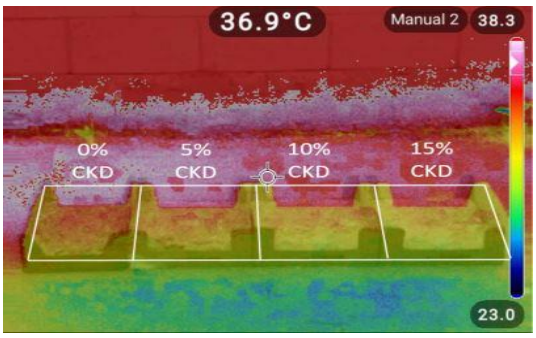

Figure 31. A thermal image of the small-scale model of the slope showing the temperature on the surface at 4:30 pm

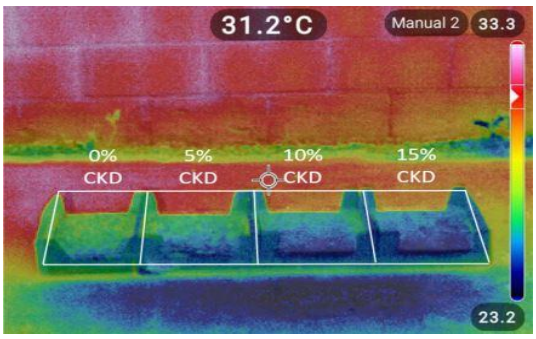

Figure 32. A thermal image of the small-scale model of the slope showing the temperature on the surface at 5:30 pm

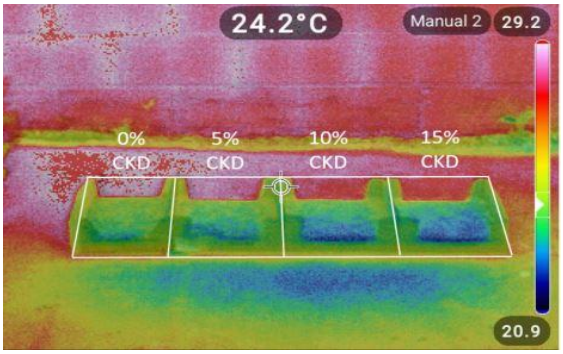

Figure 33. A thermal image of the small-scale model of the slope showing the temperature on the surface at 6:30 pm

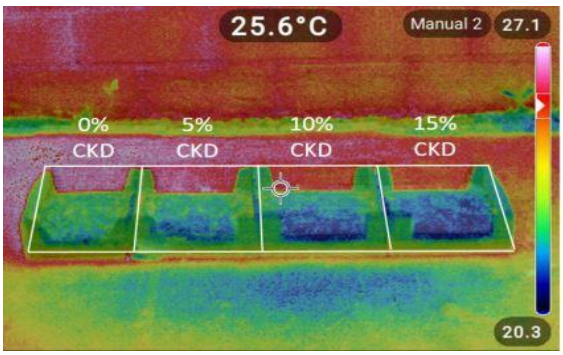

Figure 34. A thermal image of the small-scale model of the slope showing the temperature on the surface at 7:30 pm

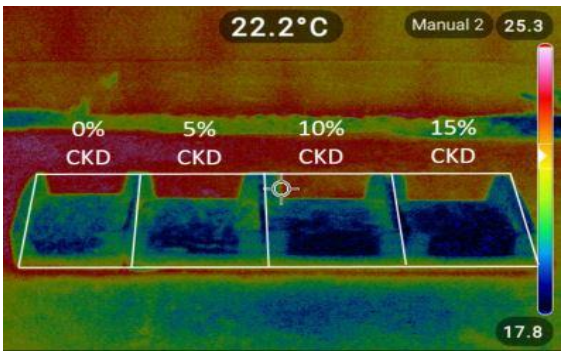

Figure 35. A thermal image of the small-scale model of the slope showing the temperature on the surface at 8:30 pm

This investigation's main goal is to monitor treated soil's thermal behavior in the field and simulated conditions for a small-scale test model. Figure 36 represents the average temperature of the slope surface for each section during the study. Soil with different amounts of additive materials is defined with different colors.

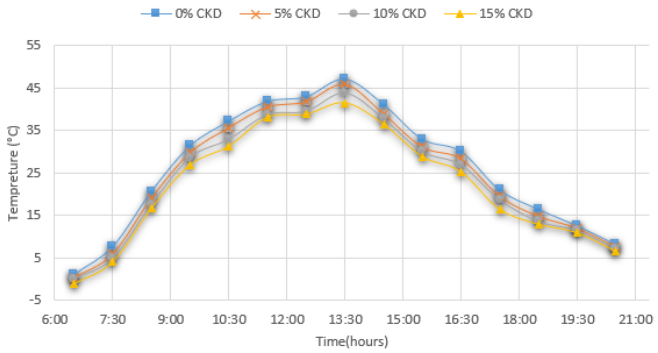

Figure 36. Surface temperature of the natural slope from 6:30 am to 8:30 pm

As seen in thermal images of soil, the slope's temperature is more considerable in soil without additive materials, and its temperature decreases by stabilizing it with CKD. Similar results were obtained for the small-scale test model. Figure 37 shows that soil diffusivity is decreasing by an increase in CKD content. Furthermore, soil with the highest CKD content has the highest thermal conductivity.

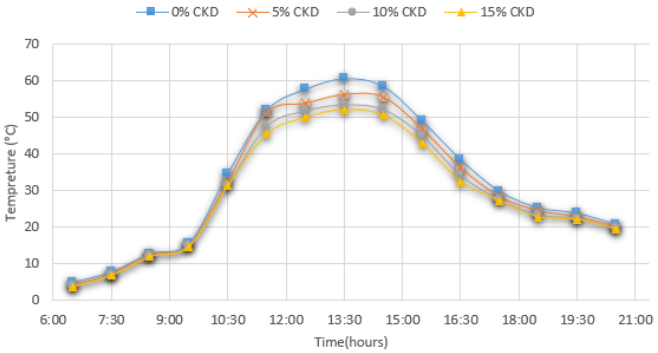

Figure 37. Surface temperature of the small-scale test model from 6:30 am to 8:30 pm

IV. CONCLUSION

The relationship between the CKD content in a natural soil slope treated with different amounts of CKD and the temperature distribution in thermal images of the slope captured in twelve hours was studied. Besides, a small-scale test model was built and used to verify the field results. The temperature of the regions with a higher CKD content is lower, which means CKD increases the soil's thermal conductivity. Additionally, CKD affects soil diffusivity. Furthermore, it is concluded that thermal image analysis can be used as an effective method to determine the distribution of additives like CKD in the stabilized soils in conjunction with the traditional techniques.

ACKNOWLEDGMENT

This research was funded by the mineral engineering department of the New Mexico Institute of Mining and Technology. The authors gratefully acknowledge the support of the mineral engineering department.

REFERENCES

[1] Abu-hamdeh, N., & Reeder, R. C. (2000). Soil thermal conductivity: effects of density, moisture, salt concentration, and organic matter. *Soil Science Society of America Journal*, *64*(4), 1285–1290. https://doi.org/10.2136/sssaj2000.6441285x

[2] Edet, C. O., Ushie, P. O., & Ekpo, C. M. (2017). Effect of additives on the thermal conductivity of loamy soil in cross river university of technology (crutech) farm, Calabar, Nigeria. *Asian Journal of Physical and Chemical Sciences*, *3*(4), 1–8. https://doi.org/10.9734/AJOPACS/2017/36665

[3] Faramarzi, L., Rasti, A., & Abtahi, S. M. (2016). An experimental study of the effect of cement and chemical grouting on the improvement of the mechanical and hydraulic properties of alluvial formations. *Construction and Building Materials*, *126*. https://doi.org/10.1016/j.conbuildmat.2016.09.006

[4] Folaranmi, J. (2009). Effect of additives on the thermal conductivity of clay. *Leonardo Journal of Sciences*, *8*(14), 74–77.

[5] Hopmans, J. W., & Dane, J. H. (1986). Thermal conductivity of two porous media as a function of water content, temperature, and density. *Soil Science*, *142*(4), 187–195. https://doi.org/10.1097/00010694-198610000-00001

[6] Kang, X., Ge, L., Kang, G., & Mathews, C. (2015). Laboratory investigation of the strength, stiffness, and thermal conductivity of fly ash and lime kiln dust stabilized clay subgrade materials. *Road Materials and Pavement Design*, *16*(4), 928–945. https://doi.org/https://doi.org/10.1080/14680629.2015.1028970

[7] Kodikara, J., Rajeev, P., & Rhoden, N. J. (2011). Determination of thermal diffusivity of soil using infrared thermal imaging. *Canadian Geotechnical Journal*, *48*(8), 1295–1302. https://doi.org/10.1139/T11-036

[8] Ochsner, T. E., Horton, R., & Ren, T. (2001). A new perspective on soil thermal properties. *Soil Science Society of America Journal*, *65*(6), 1641–1647. https://doi.org/https://doi.org/10.2136/sssaj2001.1641

[9] Rao, P. (2008). Infrared thermography and its applications in civil engineering. *The Indian Concrete Journal*, 41–50.

[10] Sabri, N. syazwani ahmad, Zakaria, Z., Mohamad, S. eva, Jaafar, A. bakar, & Hara, H. (2018). Importance of soil temperature for the growth of temperate crops under a tropical climate and functional role of soil microbial diversity. *Microbes and Environments*, *33*(2), 144–150. https://doi.org/10.1264/jsme2.ME17181

[11] Shiozawa, S., & Campbell, G. S. (1990). Soil thermal conductivity. *Remote Sensing Reviews*, *5*(1), 301–310. https://doi.org/10.1080/02757259009532137

[12] Zhang, L., Gustavsen, A., Jelle, B. P., Yang, L., Gao, T., & Wang, Y. (2017). Thermal conductivity of cement stabilized earth blocks. *Construction and Building Materials*, *151*(1), 504–511. https://doi.org/https://doi.org/10.1016/j.conbuildmat.2017.06.047

How to Cite this Article:

Adarmanabadi, H. R., Rasti, A. & Razavi, M. (2020). Thermal Image Analysis of a Cement Kiln Dust Treated Slope. International Journal of Science and Engineering Investigations (IJSEI), 9(107), 29-36. http://www.ijsei.com/papers/ijsei-910720-05.pdf